Microelectronic Engineering 87 (2010) 1220–1222

Contents lists available at ScienceDirect

Microelectronic Engineering

journal homepage: www.elsevier.com/locate/mee

# CMOS integrated radio frequency dome resonator

Wenzhe Zhou [a,*], Joshua D. Cross [b], Maxim Zalalutdinov [c], Bojan Ilic [d], Jeffrey W. Baldwin [c], Brain H. Houston [c], Harold G. Craighead [e], Jeevak M. Parpia [b]

[a] School of Electrical and Computer Engineering, Cornell University, Ithaca, NY 14853, United States
[b] Laboratory of Atomic and Solid State Physics (LASSP), Physics Department, Cornell University, Ithaca, NY 14853, United States
[c] US Naval Research Laboratory, Washington, DC 20375, United States
[d] Cornell Nanoscale Science and Technology Facility (CNF), Cornell University, Ithaca, NY 14853, United States
[e] School of Applied and Engineering Physics, Cornell University, Ithaca, NY 14853, United States

A R T I C L E  I N F O

*Article history:*
Received 18 September 2009
Received in revised form 13 November 2009
Accepted 29 November 2009
Available online 16 December 2009

*Keywords:*
MEMS resonator
CMOS–MEMS integration
Radio frequency
High Q

A B S T R A C T

Resonant RF MEMS structures can offer excellent performance for integrated sensing and RF signal processing applications. MEMS devices offer small size and low power consumption and improved physical parameters such as FQ product; however, significant impediments to a large scale commercial adoption include: production cost, difficulty of implementation and signal transduction. In this paper, we developed a generic pathway for CMOS–MEMS integration by designing MEMS dome resonators in multiple layers of stacked polycrystalline silicon in standard CMOS back end of line process and demonstrate the quality factor of dome resonator both optically and electrically. In this work, we report the highest FQ product of integrated resonator at micron level using commercial CMOS technology and the lowest operation power.

© 2009 Elsevier B.V. All rights reserved.

## 1. Introduction

Resonant radio frequency (RF) MEMS structures are of great interest as they can offer excellent performance for integrated sensing [1] and RF signal processing applications [2–4]. MEMS devices offer small size and low power consumption and improved physical parameters such as FQ product; however, significant impediments to a large scale commercial adoption include production cost, difficulty of implementation and signal transduction [5]. Ubiquitous MEMS fabricated under the standard fabrication rules of CMOS foundries are one way to achieve the potential low cost of these devices [5,6].

In this paper, we developed a generic pathway for CMOS–MEMS integration by designing MEMS dome resonators [4,7–9] in multiple layers of stacked polycrystalline silicon in the standard CMOS back end of line (BEOL) processes and to show the feasibility and reliability of the post-CMOS releasing by demonstrating the high quality factor (Q) resonators both optically and electrically.

## 2. Design and fabrication

In this work, we have designed and have fabricated RF dome resonator in a commercial CMOS process (AMIS ABN 1.5 μm) provided by ON Semiconductor® (former AMI) through The MOSIS Service without changing any steps (Fig. 1). The dome resonator was designed with an integrated transimpedance amplifier (TIA), the transresistance of which is 1 kΩ. The TIA was composed of three stages, a first common-gate (CG) stage, a second common-source stage and followed by a buffer for 50 ? impedance matching [10]. The dome readout capacitor is connected in parallel to the source resistor of CG stage (Fig. 2). The simulation of the TIA circuits in cadence (Fig. 2) proves our design with a cut-off frequency of 100 MHz. The TIA is aimed to amplify the fundamental mode signal of the dome resonator which has a higher amplitude and more practical than high order harmonic mode for sensing application. Furthermore, a chip layout of the whole design (Fig. 3a) shows that our dome resonator is quite area-efficient compared to the CMOS process we used.

Unlike the state-of-art CMOS process technology using Shallow Trench Isolation (STI) as field isolation, the early technology node CMOS process we used fabricating MEMS resonator is based on local oxidation (LOCOS) isolation. The integrated dome resonator is different from the discrete one we reported [7–9], as it has a natural three-dimensional surface curvature (Fig. 3b) similar to that at the edges of FOX derived from LOCOS, which is well known as "bird beak" shape due to lateral oxidation under the nitride mask [11].

In the post-CMOS processes, we use photoresist to protect the surrounded CMOS TIA, and lithographically define etch orifices in the top polycrystalline silicon layer that comprises the dome resonator when the underlying oxide layer is removed by wet etch in

* Corresponding author. Tel.: +1 607 220 7905.
*E-mail address:* wz85@cornell.edu (W. Zhou).

0167-9317/$ - see front matter © 2009 Elsevier B.V. All rights reserved.
doi:10.1016/j.mee.2009.11.157

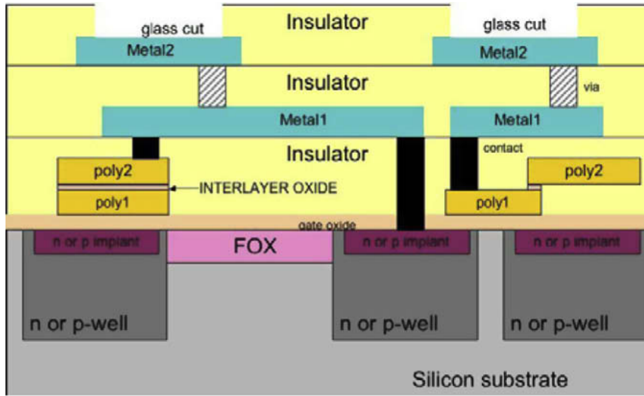


**Fig. 1.** Schematic of the CMOS–MEMS sequence with AMIS ABN 1.5 μm process provided by The MOSIS Service.

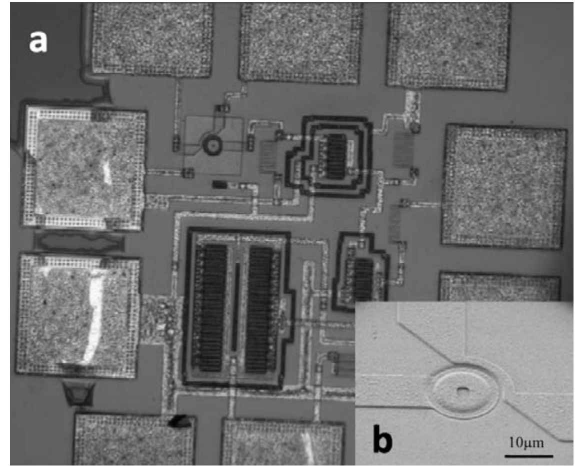


**Fig. 3.** (a) Image of integrated MEMS–CMOS chip after the post-CMOS processes (b) (inset) SEM image of integrated polycrystalline silicon dome resonator which located on the upper left corner of the chip in image (a).

buffered oxide etchant to create the dome cavity. The 320 nm top polycrystalline silicon layer is then etched by $CF_4$ plasma gas in reactive ion etching (RIE) for 55 min and a sequent wet etching in BOE is conducted for another 50 min to release the 55-nm-thick inter-polycrystalline-silicon oxide layer (Fig. 4) through the orifice we opened after CMOS process.

## 3. Experiment results and discussion

The released dome resonator (Fig. 3b) can be driven by a 405 nm-wavelength diode laser modulated by RF signal and its motion can be detected by a 633 nm-wavelength He–Ne laser [12]. Based on this method, we have reported the dome resonator with quality factor as high as 8000 under vacuum [7]. With similar motion detecting method but using resistive actuation, a quality factor of 2500 was achieved as a reasonable trade-off for integration [8]. In order to seek a feasible actuation of CMOS integrated dome resonator, we design the surround heater which is connected to the dome resonator. The generated heat is conducted to both top and bottom polycrystalline silicon layer of dome resonator and

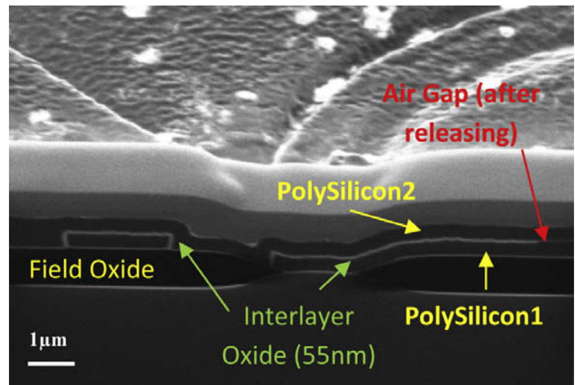


**Fig. 4.** Focused ion beam (FIB) cross-section image of the integrated dome resonator.

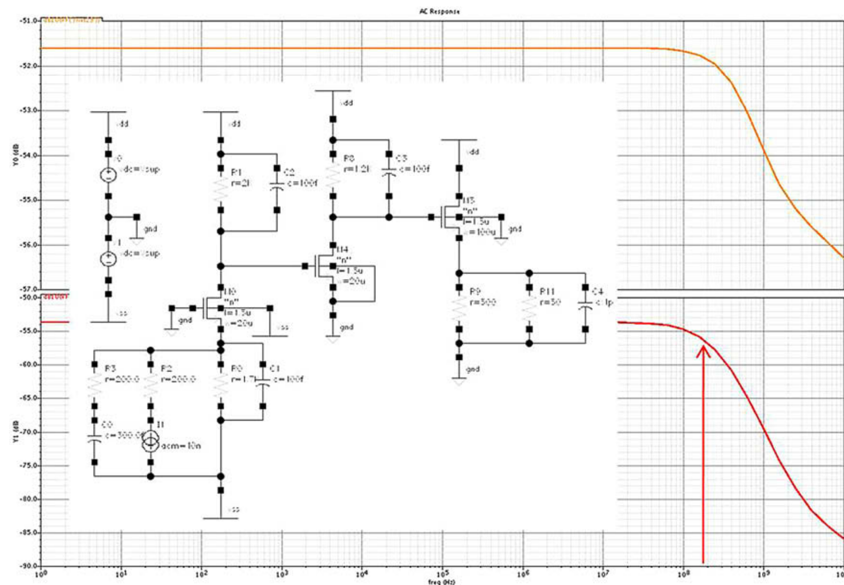


**Fig. 2.** The circuit schematic of the three stage common-gate transimpedance amplifier with a cut-off frequency of 100 MHz (pointed by the arrow).

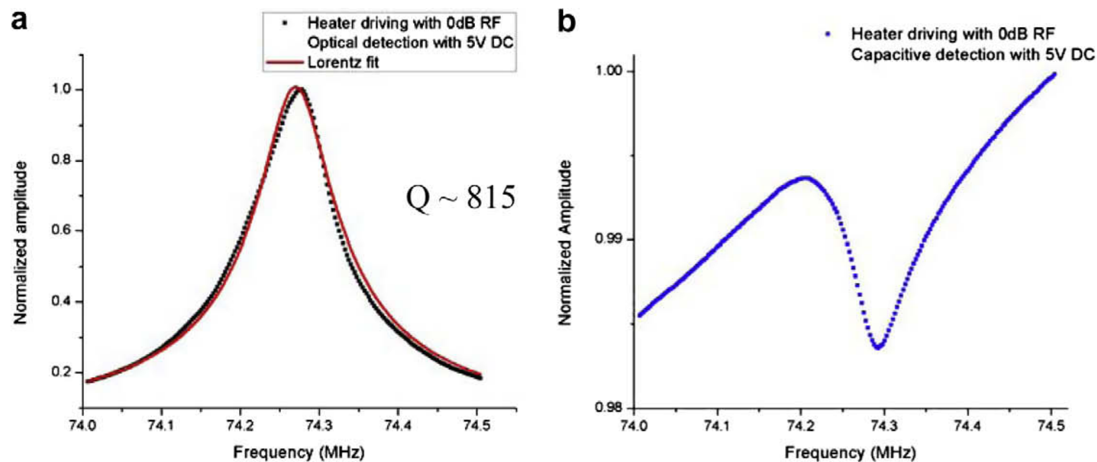


**Fig. 5.** (a) (Left) frequency response of thermally driven integrated dome resonator with high Q detected by 632.8 nm He–Ne laser, (b) (right) frequency response of thermally driven integrated dome resonator using capacitive detection.

thus drives the resonator. With these designed integrated heater pads, we resistively drove the dome resonator and optically detected a Q more than 800 (Fig. 5a), which is quite reasonable compared to a Q around 2000 obtained by the same resonator through laser driving. Even though the quality factor is not as high as our previous device due to the constraints of the mechanical properties of polycrystalline silicon layer inherited from MOSIS and the intrinsic mechanical properties of a naturally buckle grown polycrystalline silicon, the resonator already shown great sensitivity. The competitive FQ product of $6 \times 10^{10}$ is the highest compared with other reported integrated resonators at micron level using commercial CMOS process [13]. To certain technology node, the dome resonator is still scalable and we can foresee the great potential of this device to achieve even higher FQ product as the feature size drops [14].

Cross et al. [15] recently reported the piezoresistive transduction in multilayer polycrystalline silicon resonators, and the interlayer dielectric is the major leakage source for dissipation of electrical energy. The CMOS-standard high quality oxide thin film decides the efficiency of the transfer of electrical energy to mechanical energy. Besides, our dome resonator, the fundamental mode require low energy budget in thermally driving case, which best explain why the operation power of the dome resonator is the lowest among all reported CMOS–MEMS integrated resonator [13], DC bias as low as 5 V. The easy driving and low power consumption features of this dome resonator are highly applicable in radio frequency front-end circuits. Using sensitive capacitive method [16,17], we got the electrical readout of the dome resonator working great at the same resonant frequency (Fig. 5b), which shows a high feasibility of harnessing MEMS resonator within CMOS technology.

## 4. Conclusion

We demonstrate the approach to mass producing RF MEMS resonators with a standard MOSIS technology, harnessing the integration of resonant MEMS devices into CMOS integrated circuits. The integrated dome resonators that we designed show excellent high quality factor ($Q \sim 800$–1000) in vacuum at rather low operation power and achieve the highest FQ product for integrated resonator using commercial CMOS process. The dome resonators have already been made to be nonlinear micromechanical mixer and filter [18] and the new results propose even broader applications of the dome resonator as candidate for next generation low operation power CMOS compatible radio frequency front-end circuits. This may also extend the dome resonators to work as portable integrated devices for chemical and biological sensing [19].

## Acknowledgements

The author (W.Z.) would like to thank Dr. Robert B. Reichenbach of ESI Inc. for helpful discussion and appreciate Mick Thomas of Cornell Center for Materials Research (CCMR) for the help of FIB imaging. The work is supported by DARPA MTO (Grant HR 0022-06-1-0042) and by the Office of Naval Research. Fabrication was performed in part at the Cornell Nanoscale Science and Technology Facility (CNF), a member of the National Nanotechnology Infrastructure Network, which is supported by the National Science Foundation (Grant ECS-0335765).

## References

[1] B. Ilic, H.G. Craighead, S. Krylov, W. Senaratne, C. Ober, P. Neuzil, J. Appl. Phys. 95 (2004) 3694–3703.
[2] C.T.-C. Nguyen, L.P.B. Katehi, G.M. Rebeiz, Proc. IEEE 86 (1998) 1756–1768.
[3] C.T.-C. Nguyen, IEEE CICC (2004) 257–264.
[4] R.B. Reichenbach, Ph.D. Thesis, Cornell University, 2006.
[5] G.K. Fedder, R.T. Howe, T.-J.K. Liu, E.P. Quévy, Proc. IEEE 96 (2008) 306–322.
[6] G. Villanueva, F. Perez-Murano, M. Zimmermann, J. Lichtenberg, J. Bausells, Microelectron. Eng. 83 (2006) 1302–1305.
[7] M. Zalalutdinov, K.L. Aubin, C. Michael, R.B. Reichenbach, T. Alan, A.T. Zehnder, B.H. Houston, J.M. Parpia, H.G. Craighead, Proc. SPIE 5116 (2003) 229–236.
[8] M. Zalalutdinov, K.L. Aubin, R.B. Reichenbach, A.T. Zehnder, B. Houston, J.M. Parpia, H.G. Craighead, Appl. Phys. Lett. 83 (2003) 3815–3817.
[9] R.B. Reichenbach, M.K. Zalalutdinov, K.L. Aubin, D.A. Czaplewski, B. Ilic, B.H. Houston, H.G. Craighead, J.M. Parpia, Proc. SPIE 5344 (2004) 51–58.
[10] M. Zalalutdinov, J. Cross, J. Baldwin, B. Ilic, W. Zhou, B. Houston, J. Parpia, J. Microelectromech. Syst., accepted for publication.
[11] J.D. Plummer, M.D. Deal, P.R. Griffin, Silicon VLSI Technology: Fundamentals, Practice and Modeling, Prentice Hall Inc., 2000.
[12] S.S. Verbridge, D.F. Shapiro, H.G. Craighead, J.M. Parpia, Nano Lett. 7 (2007) 1728–1735.
[13] J.L. Lopez, J. Verd, J. Teva, G. Murillo, J. Giner, F. Torres, A. Uranga, G. Abadal, N. Barniol, J. Micromech. Microeng. 19 (2009) 015002.
[14] M. Li, H.X. Tang, M.L. Roukes, Nat. Nanotechnol. 2 (2007) 114–120.
[15] J.D. Cross, B.R. Ilic, M.K. Zalalutdinov, W. Zhou, J.W. Baldwin, B.H. Houston, H.G. Craighead, J.M. Parpia, Appl. Phys. Lett. 95 (2009) 133113.
[16] P.A. Truitt, J.B. Hertzberg, C.C. Huang, K.L. Ekinci, K.C. Schwab, Nano Lett. 7 (2007) 120–126.
[17] R.B. Reichenbach, M. Zalalutdinov, J.M. Parpia, H.G. Craighead, IEEE Electron Dev. Lett. 27 (2006) 805–807.
[18] R.B. Reichenbach, M. Zalalutdinov, K.L. Aubin, R. Rand, B.H. Houston, J.M. Parpia, H.G. Craighead, J. Microelectromech. Syst. 14 (2005) 1244–1252.
[19] P.S. Waggoner, M. Varshney, Lab Chip (2009) 3095–3099.